

Thermal and electrical studies on mixed crystals of $\text{Cu}_x\text{Zn}_{1-x}(\text{HCOO})_2 \cdot 2\text{H}_2\text{O}$

M. G. EI-SHAARAWY*, S. A. SHAMA†

Departments of *Physics and †Chemistry, Faculty of Science, Zagazig University, Benha, Egypt

E-mail: mousa@intouch.com

The electrical properties of $\text{Cu}_x\text{Zn}_{1-x}(\text{HCOO})_2 \cdot 2\text{H}_2\text{O}$ have been studied over a temperature range of 78–400 K. Results of the electrical conductivity, $\sigma_{\text{d.c.}}$, $\sigma_{\text{a.c.}}$, thermoelectric power, θ , relative permittivity, ϵ'_r , and dielectric loss factor, ϵ''_r , were reported. Anomalies in the physical properties have been observed at 220 K and at the vicinity of the decomposition temperature, and the mechanism of decomposition of solids has been studied. A random nucleation process (A_3) was found to be the predominant decomposition mechanism for the system investigated. The effects of chemical composition and crystal structure on the physical properties are discussed. © 1999 Kluwer Academic Publishers

1. Introduction

Due to the importance of organic compounds in many branches of technology, such as electronic devices and active materials, much effort has recently been devoted to relating the chemical and crystal structure of these compounds to their physical properties [1–4]. There are many papers dealing with the thermal decomposition of organic acids and their salts, but still not enough information has been reported about the thermal effect on the physical properties of mixed salts of organic acids, especially their electrical properties.

The metal formate dihydrate $\text{M}(\text{HCOO})_2 \cdot 2\text{H}_2\text{O}$ ($\text{M} = \text{Mg}, \text{Mn}, \text{Fe}, \text{Ni}, \text{Cu}, \text{Zn}, \text{Cd}$) occurs in the isostructural monoclinic system, with space group $P2_1/C$ [5]. It has been established that isostructural salts of $\text{Cu}(\text{HCOO})_2 \cdot 2\text{H}_2\text{O}$ and $\text{Zn}(\text{HCOO})_2 \cdot 2\text{H}_2\text{O}$ form a discontinuous solid solution series, where the metal ions occupy one of the two available positions [$\text{M}(1)$ and $\text{M}(2)$] of non-equivalent centres of symmetry. The cation at the $\text{M}(1)$ -site is co-ordinated by six oxygen atoms from formate ions $(\text{HCOO})^-$, while the metal ion at the $\text{M}(2)$ -site is co-ordinated by four water molecules and two oxygen atoms from formate ions [5].

The present investigation concerns the effect of chemical composition and heat on the physical properties of $\text{Cu}_x\text{Zn}_{1-x}(\text{HCOO})_2 \cdot 2\text{H}_2\text{O}$: such as crystal structure, electrical conductivity, $\sigma_{\text{a.c.}}$, $\sigma_{\text{d.c.}}$, Seebeck coefficient, θ , relative permittivity constant, ϵ'_r , dielectric loss factor, ϵ''_r , and thermal stability.

2. Experimental procedure

All chemicals used in this work were of analytical grade (BDH). Pure and mixed metal formates were prepared from basic copper carbonate, zinc oxide and formic acid using a method reported elsewhere [5]. The solid

products were washed with alcohol and dried in air. The chemical composition of $\text{Cu}_x\text{Zn}_{1-x}(\text{HCOO})_2 \cdot 2\text{H}_2\text{O}$ ($x = 0, 0.11, 0.22, 0.51, 0.73, 0.91$ and 1.0) was determined by means of elemental analysis of C and H, and by atomic absorption for Zn and Cu.

To identify the composition of the products, infrared (i.r.) spectra for the investigated samples were recorded using a Perkin-Elmer 32 spectrophotometer, KBr disc and Nujol oil nulls. The product spectra show strong absorption bands at 1660–1615 and 1360–1320 cm^{-1} due to asymmetric and symmetric carboxylate stretching vibrations, indicating the formation of metal–carboxylate bonds [6]. The bands that appear at 1000–200 cm^{-1} for the metal formates are a good assignment for the metal–oxygen vibrations.

To determine the crystal structure of the investigated system X-ray diffraction (XRD) patterns of the sample were carried out with the aid of a Phillips unit, type PW 210 311, using a copper target and a Ni filter. The lattice parameters for $\text{Cu}_x\text{Zn}_{1-x}(\text{HCOO})_2 \cdot 2\text{H}_2\text{O}$ showed the formation of an isostructural monoclinic system for the entire compositional range. These results agree well with those reported by Stoilova and Gentcheva [5].

Electrical measurements (d.c.- and a.c.-conductivity, $\sigma_{\text{d.c.}}$, $\sigma_{\text{a.c.}}$, respectively; relative permittivity, ϵ'_r ; dielectric loss factor, ϵ''_r ; and Seebeck voltage coefficient, θ) were carried out on pellets 7 mm in diameter and approximately 1 mm thick, pressed under a pressure of 1800 kg cm^{-2} . The two parallel surfaces of each pellet were coated with silver paint (BDH) and checked for good conduction. The dependence of the electrical properties on the temperature was studied carefully in a cryostat at a temperature range of 78–400 K. The resistivity of the pellets was measured using a Keithly Electrometer model 610. Measurements under the a.c. field were performed at various frequencies ranging

* Author to whom correspondence should be addressed.

from 10^2 – 10^6 Hz using LCR model SRS 720 (USA). Seebeck voltage measurements were carried out at temperature intervals of approximately 40 K.

Thermal analyses (thermogravimetric and differential thermal analyses TGA and DTA, respectively) were conducted in air atmosphere using a Shimadzu model 30 thermal analyser at a heating rate of 10 K min^{-1} , using a 6 mg sample to ensure linear heating rate.

3. Results and discussion

The DTA and TGA thermal analyses for $\text{Cu}_x\text{Zn}_{1-x}(\text{HCOO})_2 \cdot 2\text{H}_2\text{O}$ samples showed similar behaviour, in which decomposition occurs in a single-stage process (TGA) due to separation of water, and is accompanied by an endothermic peak (DTA). The data are summarized and given in Table I, from which it can be seen that the thermal stability of the mixed salts is higher than that of pure salts. For a single heating rate, the fraction of solid decomposed, α , at temperature, T , can be used to determine the kinetics of decomposition and their mechanisms for both the mixed and pure salts. This can be done by applying the linear regression analysis method to particular mathematical relationships associated with the kinetic mechanism model, $F(\alpha)$ [7]. The best correlation factor obtained is then used to define the most probable kinetic mechanism for decomposition. For our system the best fit was obtained by a random nucleation process (A_3). According to this mechanism, nucleation of decomposed solid is a random process. As nuclei grow larger, they must eventually impinge on one another, so that growth ceases where the crystals touch. The kinetic data for the random nucleation process are summarized and listed in Table II. It can be seen that the activation energy of the decomposition process in the mixed salts is higher than that in the pure ones.

TABLE I Thermal analysis data for the $\text{Cu}_x\text{Zn}_{1-x}(\text{HCOO})_2 \cdot 2\text{H}_2\text{O}$ system

Sample composition	Peak temperature (K)	Thermal nature	Weight loss (%)
$\text{Zn}(\text{HCOO})_2 \cdot 2\text{H}_2\text{O}$	328	Endothermic	23.48
$\text{Cu}_{0.11}\text{Zn}_{0.89}(\text{HCOO})_2 \cdot 2\text{H}_2\text{O}$	331	Endothermic	23.43
$\text{Cu}_{0.32}\text{Zn}_{0.68}(\text{HCOO})_2 \cdot 2\text{H}_2\text{O}$	335	Endothermic	23.42
$\text{Cu}_{0.51}\text{Zn}_{0.49}(\text{HCOO})_2 \cdot 2\text{H}_2\text{O}$	346	Endothermic	23.38
$\text{Cu}_{0.73}\text{Zn}_{0.27}(\text{HCOO})_2 \cdot 2\text{H}_2\text{O}$	358	Endothermic	23.34
$\text{Cu}_{0.91}\text{Zn}_{0.09}(\text{HCOO})_2 \cdot 2\text{H}_2\text{O}$	340	Endothermic	23.31
$\text{Cu}(\text{HCOO})_2 \cdot 2\text{H}_2\text{O}$	323	Endothermic	23.26

TABLE II Kinetic parameters for thermal dehydration of $\text{Cu}_x\text{Zn}_{1-x}(\text{HCOO})_2 \cdot 2\text{H}_2\text{O}$ using the kinetic model of random nucleation

Sample composition	E (eV)	$\ln A$ (s^{-1})	r (correlation factor)
$\text{Zn}(\text{HCOO})_2 \cdot 2\text{H}_2\text{O}$	1.06	1.6×10^{10}	0.9992
$\text{Cu}_{0.11}\text{Zn}_{0.89}(\text{HCOO})_2 \cdot 2\text{H}_2\text{O}$	1.14	1.9×10^{10}	0.9998
$\text{Cu}_{0.32}\text{Zn}_{0.68}(\text{HCOO})_2 \cdot 2\text{H}_2\text{O}$	1.27	2.1×10^{10}	0.9989
$\text{Cu}_{0.51}\text{Zn}_{0.49}(\text{HCOO})_2 \cdot 2\text{H}_2\text{O}$	1.40	3.4×10^{10}	0.9994
$\text{Cu}_{0.73}\text{Zn}_{0.27}(\text{HCOO})_2 \cdot 2\text{H}_2\text{O}$	1.46	6.1×10^{10}	0.9996
$\text{Cu}_{0.91}\text{Zn}_{0.09}(\text{HCOO})_2 \cdot 2\text{H}_2\text{O}$	1.56	9.1×10^{10}	0.9995
$\text{Cu}(\text{HCOO})_2 \cdot 2\text{H}_2\text{O}$	1.04	1.1×10^{10}	0.9993

Since all the investigated salts have the same crystal structure, so the increase in the decomposition rate found in the mixed salts could be attributed to the autocatalytic effect of the solid product phase and their subsequent growth via a reaction interface. In general, however, and wherever a reaction interface is involved, the difference in volume between solid reactants and the solid product leads to production of a strained structure. This strained structure produces fragmentation of the original particles, causing active solids that can be recognized by their high chemical reactivity depending on the type and the volume of the product nuclei.

The I–V characteristics for $\text{Zn}_x\text{Cu}_{1-x}(\text{HCOO})_2 \cdot 2\text{H}_2\text{O}$ samples were investigated at room temperature under conditions of rising and falling voltage in the range 10^2 – $5 \times 10^3 \text{ V cm}^{-1}$. The data were found to fit the $\log I$ – $\log V$ dependence with $n \sim 1$, indicating that these compounds obey Ohm's law. In order to check the type of electrical conduction in our system, resistance was measured as a function of time at room temperature by applying a constant voltage of 300 V (i.e. approximately 3000 V cm^{-1}) for 3 h. The resistance was found to be constant with time, which is evidence that there is no measurable polarization effect and suggests that conduction in these samples is mainly electronic. This could be supported by the Seebeck voltage measurements, which showed negative values for all samples under investigation, Table III.

The temperature dependence of conductivity, $\sigma_{\text{d.c.}}$, for the samples investigated is shown in Fig. 1, as a plot of $\ln \sigma_{\text{d.c.}}$ versus T^{-1} . The plots show abrupt changes in $\sigma_{\text{d.c.}}$ values at temperatures of approximately 220 K and the dissociation temperature, T_b . T_b was found to depend on the composition of the sample and coincides well with its decomposition temperature as enhanced by the DTA thermograph. On the other hand the discontinuity in $\sigma_{\text{d.c.}}$ values at 220 K is independent of the composition of the samples, which having the same crystal structure at room temperature, therefore it could be attributed to a phase transition occurring in the samples at this temperature. At temperatures lower than 220 K, $\sigma_{\text{d.c.}}$ was found to decrease slightly with increasing T , referring to metallic behaviour. While in

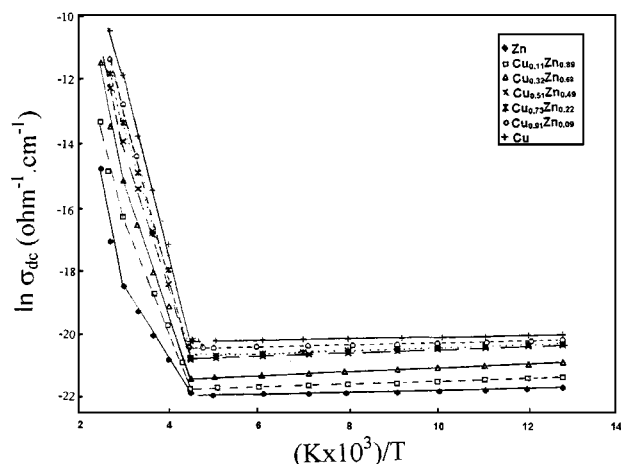


Figure 1 Effect of temperature on the d.c.-electrical conductivity of $\text{Cu}_x\text{Zn}_{1-x}(\text{HCOO})_2 \cdot 2\text{H}_2\text{O}$ samples.

TABLE III Conductivity data for the $\text{Cu}_x\text{Zn}_{1-x}(\text{HCOO})_2 \cdot 2\text{H}_2\text{O}$ system

Sample composition	$\sigma_{\text{d.c.}}$ at 300 K ($\Omega^{-1} \text{cm}^{-1}$)	E (eV)	θ ($\mu\text{V K}^{-1}$)	s
$\text{Zn}(\text{HCOO})_2 \cdot 2\text{H}_2\text{O}$	3.6×10^{-9}	0.22	-46	0.44 ± 0.06
$\text{Cu}_{0.11}\text{Zn}_{0.89}(\text{HCOO})_2 \cdot 2\text{H}_2\text{O}$	2.1×10^{-8}	0.31	-58	0.49 ± 0.11
$\text{Cu}_{0.32}\text{Zn}_{0.68}(\text{HCOO})_2 \cdot 2\text{H}_2\text{O}$	5.3×10^{-8}	0.35	-66	0.54 ± 0.08
$\text{Cu}_{0.51}\text{Zn}_{0.49}(\text{HCOO})_2 \cdot 2\text{H}_2\text{O}$	1.5×10^{-7}	0.39	-75	0.47 ± 0.05
$\text{Cu}_{0.73}\text{Zn}_{0.27}(\text{HCOO})_2 \cdot 2\text{H}_2\text{O}$	3.1×10^{-7}	0.40	-78	0.52 ± 0.07
$\text{Cu}_{0.91}\text{Zn}_{0.09}(\text{HCOO})_2 \cdot 2\text{H}_2\text{O}$	4.0×10^{-7}	0.43	-86	0.61 ± 0.05
$\text{Cu}(\text{HCOO})_2 \cdot 2\text{H}_2\text{O}$	8.4×10^{-7}	0.46	-94	0.53 ± 0.11

the range of $220 < T < T_b$, semiconducting behaviour is obtained, where $\sigma_{\text{d.c.}}$ satisfies the equation

$$\sigma = \sigma_0 \exp(-E_a/kT)$$

where σ_0 is constant, E_a is the activation energy and k is the Boltzmann constant. The d.c.-conductivity data are summarized in Table III. It is noticed that the $\sigma_{\text{d.c.}}$ value increases with increasing Cu content in the sample. The electrical conductivity, $\sigma_{\text{d.c.}}$, is attributed to the drift of charge carriers, which is given by the formula [8]

$$\sigma_{\text{d.c.}} = ne\mu$$

where e is the electronic charge, n and μ are the concentration and the mobility of the charge carriers, respectively. n can be calculated according to [9]

$$n = 2(2\pi m^*kT/h^2)^{3/2} \exp(-E_a/kT)$$

where m^* is the effective mass of the charge carrier, and is assumed to be equal to the mass of the rest of the electron. The calculated room temperature values of n lie in the range 10^{17} – 10^{21} . The value of the mobility, μ , lies in the range 10^{-3} – $10^{-9} \text{cm}^2 \text{V}^{-1} \text{s}^{-1}$. A value of μ that is much smaller than approximately $1 \text{cm}^2 \text{V}^{-1} \text{s}^{-1}$ means that the band model cannot be used to describe the conduction mechanism of our system. The width of an energy band reflects the degree of overlapping of a particular set of atomic orbitals [9]. In the present case, poor overlap between the 3d orbitals of metal ions and the p orbitals of carboxylate groups is expected and, therefore, the energy band will be narrow. Now, the perturbations from the lattice vibrations are large and the carrier mobility is low. This indicates that charge transport occurs by a hopping mechanism in which the charge carriers are thermally activated and displaced to an adjacent localized state. This may have occurred by transport of the electrons from the COO^- ion to another one through Cu^{2+} ions, which can be easily changed to Cu^+ . This can also explain the increase in $\sigma_{\text{d.c.}}$ values with increasing Cu content in the sample.

The temperature dependence of $\sigma_{\text{a.c.}}$, relative permittivity, ϵ'_r , and dielectric loss factor, ϵ''_r , have been measured in the temperature range 78–400 K as a function of frequency, ω , ranging from 10^2 to 10^6 Hz. The plots of $\ln \sigma_{\text{a.c.}}$ versus T^{-1} showed similar behaviour for all samples (at typical plot is shown in Fig. 2). At lower temperatures, $\sigma_{\text{a.c.}}(\omega)$ is always higher than $\sigma_{\text{d.c.}}$, indicating the presence of barrier effects; while at higher temperatures $\sigma_{\text{a.c.}}(\omega)$ coincides with $\sigma_{\text{d.c.}}$ at all measur-

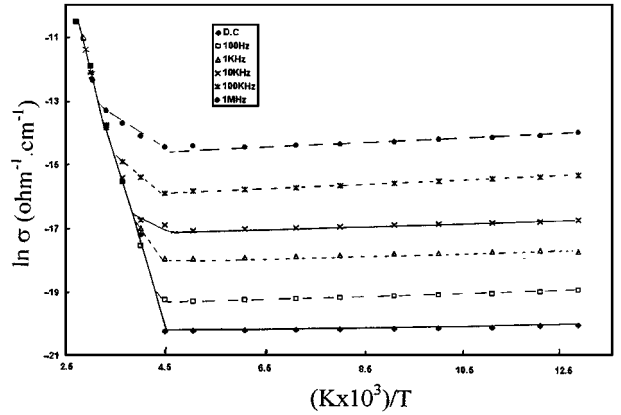


Figure 2 Correlation between $\ln \sigma$ and the reciprocal of absolute temperature at different frequencies for $\text{Cu}_x\text{Zn}_{1-x}(\text{HCOO})_2 \cdot 2\text{H}_2\text{O}$ samples.

ing frequencies. The frequency dependence of $\sigma_{\text{a.c.}}(\omega)$ obeys the relation

$$\sigma_{\text{a.c.}}(\omega) = A\omega^s$$

where A is a frequency independent parameter and the exponent s depends on the composition of the sample and has a value that lies in the range 0.38–0.66, Table III. This behaviour of a.c. conductivity suggests a hopping conduction mechanism for electrons at temperatures between 220 K and T_b [10]. It should be mentioned here that $\sigma_{\text{a.c.}}$ showed changes, at all frequencies, at the decomposition temperature of the respective compounds.

The variation of ϵ'_r and ϵ''_r with T at 50 kHz for all samples investigated is shown in Figs 3 and 4, respectively. From the figures it is clear that there are three

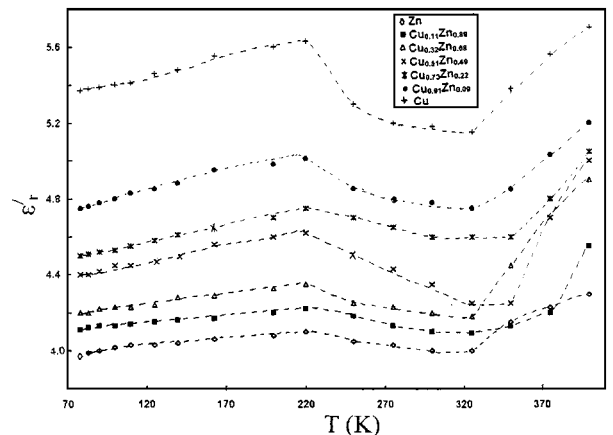


Figure 3 Effect of temperature on relative permittivity, ϵ'_r , at 50 kHz for $\text{Cu}_x\text{Zn}_{1-x}(\text{HCOO})_2 \cdot 2\text{H}_2\text{O}$ samples.

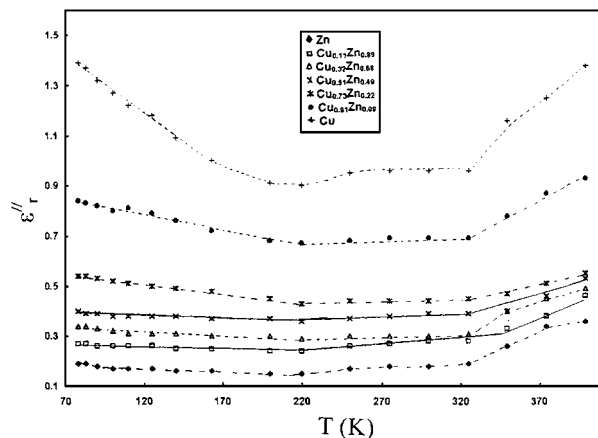


Figure 4 Effect of temperature on dielectric loss factor, ϵ'' , at 50 kHz for $\text{Cu}_x\text{Zn}_{1-x}(\text{HCOO})_2 \cdot 2\text{H}_2\text{O}$ samples.

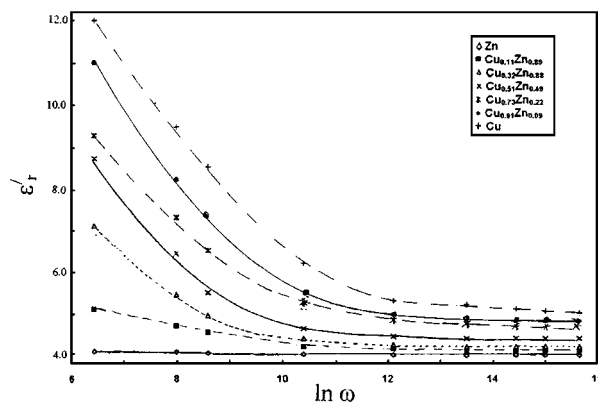


Figure 5 Correlation between relative permittivity, ϵ'_r , and $\ln \omega$ at 250 K for $\text{Cu}_x\text{Zn}_{1-x}(\text{HCOO})_2 \cdot 2\text{H}_2\text{O}$ samples.

regions distinguished by two breaks: one at $T = 220$ K (phase transition, see above) and the other at T_b , which is the dissociation temperature of the solid. The abrupt rise in ϵ'_r at the decomposition temperature may be due to large ionic polarization of the crystals, as well as to disordering effects of dipoles originating from formate ion groups and metal ions in the vicinity of the decomposition temperature.

The isothermal measurements of ϵ'_r (at $T = 250$ K) as a function of frequency for all samples investigated are shown in Fig. 5. From the figure it is shown that the dispersion of permittivity increases with increasing Cu content in the sample. This could be ascribed to the higher polarizability of Cu^{2+} compared with that of Zn^{2+} in the crystal structure investigated. Also by increasing frequency, the values of ϵ'_r will decrease, which is the general trend for such compounds. This decrease in ϵ'_r with frequency may be ascribed to fast variation of the alternating field accompanied by an applied frequency. The dipoles cannot follow such fast

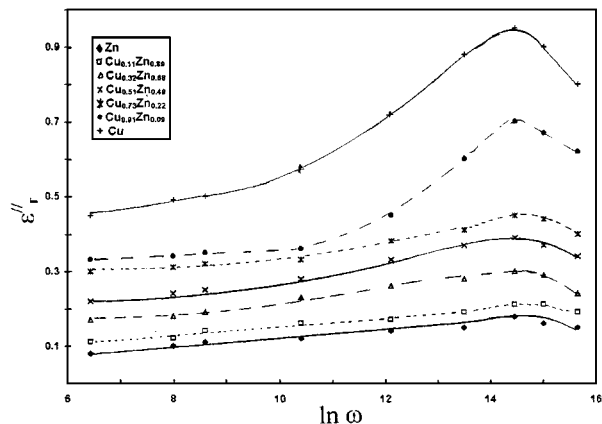


Figure 6 Correlation between dielectric loss factor, ϵ'' , and $\ln \omega$ at 250 K for $\text{Cu}_x\text{Zn}_{1-x}(\text{HCOO})_2 \cdot 2\text{H}_2\text{O}$ samples.

variation, with the result that polarizability decreases as well as ϵ'_r .

The plot of ϵ''_r against frequency, at $T = 250$ K, is shown in Fig. 6. From the figure it is noticed that for each sample ϵ''_r increases initially with increasing frequency to reach a maximum and then decreases slightly with further increase in frequency. An interesting point worth noting is that the peaks nearly occur at the same frequency, 300 kHz for all the compositions investigated. Furthermore, peak height was found to be a function of composition, such that it increases with Cu content in the sample. It should be mentioned here that the plots of ϵ''_r versus T for a frequency of 300 kHz, at which maxima are observed, also show breaks at temperatures of 220 K (phase transition, as mentioned above) and at the decomposition temperature, T_b .

References

1. K. B. R. VARMA and A. K. RAYCHAUDHURI, *J. Phys. D., Appl. Phys.* **22** (1989) 809.
2. J. TTOPFER and J. JUNG, *Thermochim. Acta* **202** (1992) 281.
3. D. CHEN, X. GAO and D. DORLIMORE, *ibid.* **215** (1993) 65.
4. C. ECOLIVET, A. MINIEWICZ and M. SANOUR, *J. Phys. Chem. Solids* **53** (1992) 511.
5. D. STOILOVA and G. GENTCHEVA, *J. Solid State Chem.* **100** (1994) 24.
6. A. G. GOYDON, "The Identification of Molecular Spectra," 4th Ed. (Wiley, New York, 1976).
7. M. A. MOUSA and A. M. SUMMAN, *Thermochim. Acta* **167** (1990) 123, and references therein.
8. M. M. ABDEL-KADER, F. EL-KABBANY and A. EL-SHAWARBY, *J. Phys. Status Solidi (a)* **127** (1991) 121.
9. K. KAO and W. HWANG, "Electrical transport in solids," (Pergamon Press, New York, 1982).
10. A. GHOSH, *Phys. Rev. B* **42** (1996) 5665.

Received 19 June

and accepted 3 September 1998